Ferro-Orbital Order and Strong Magnetic Anisotropy in the Parent Compounds of Iron-Pnictide Superconductors

Chi-Cheng Lee (李啟正),[1] Wei-Guo Yin (尹卫国),[1] and Wei Ku (顧威)[1,2]

[1]*Condensed Matter Physics and Materials Science Department, Brookhaven National Laboratory, Upton, New York 11973, USA*

[2]*Physics Department, State University of New York, Stony Brook, New York 11790, USA*

(Received 3 June 2009; published 22 December 2009)

The puzzling nature of magnetic and lattice phase transitions of iron pnictides is investigated via a first-principles Wannier function analysis of representative parent compound LaOFeAs. A rare ferro-orbital ordering is found to give rise to the recently observed highly anisotropic magnetic coupling, and drive both phase transitions—without resorting to widely employed frustration or nesting picture. The revealed necessity of the additional orbital physics leads to a correlated electronic structure fundamentally distinct from that of the cuprates. In particular, the strong coupling to the magnons advocates active roles of light orbitons in spin dynamics and electron pairing in iron pnictides.

DOI: 10.1103/PhysRevLett.103.267001 PACS numbers: 74.25.Jb, 71.15.Mb, 74.20.Mn, 74.25.Ha

With a striking similarity to the cuprate families [1], recently discovered high-temperature superconductivity in iron pnictides emerges upon suppression of magnetic order via additional charge doping [2,3]. This new example of close proximity of superconductivity to the magnetic phase has raised again the long standing questions concerning the intimate relationship between these two seemingly exclusive phases [4–15]. Following the cuprate research, a big thrust of current efforts has been to establish superconductivity in these compounds via magnetic correlations, despite the apparently diverse perspectives of the magnetism itself [4–6]. Clearly, a solid understanding of the parent compounds and their magnetism is an essential first step toward a convincing resolution of superconductivity in the doped systems, especially within the heavily discussed spin fluctuation scenario of pairing [4–15].

The parent undoped compounds of the iron pnictides have a quite unusual in-plane magnetic structure. Unlike the antiferromagnetic (AFM) magnetic moments along both the x and y directions in the copper oxides (the G-AF structure), the magnetic moments in the iron pnictides are only AFM in the x direction, but align ferromagnetically along the y direction. In the local picture, this curious stripelike (or C-AF) structure is currently explained [12–14] by requiring a strong next-nearest-neighbor (NNN) Heisenberg AFM coupling, J_2, larger than half of the nearest-neighbor (NN) AFM coupling, J_1, such that the G-AF structure favored by J_1 is suppressed energetically. The competition between C-AF and G-AF implies a strong magnetic frustration [12–14]. This frustration was argued to account for the observed small iron spin moment $\sim 0.36\mu_B$ [3] and to promote superconducting order via relief of the magnetic entropy [12]. In addition, a fluctuating electron nematic order was predicted in the spin frustration case [13] to account for the structural transition at slightly higher temperature [3], and was used to support the close relation between the physics of the cuprate and the iron-pnictide superconductors [13].

However, if the system is really that frustrated, the rather high magnetic transition temperature ($T_N \sim 137$ K) [3] would be difficult to understand. Furthermore, against the overall symmetry of the system, a surprisingly strong anisotropic NN coupling in the x and y directions was identified very recently from the inelastic neutron scattering measurements on $CaFe_2As_2$ [5], consistent with results of recent DFT calculations [4,15]. This enormous anisotropy suggests that a *strong* rotational symmetry breaking has taken place prior to the magnetic ordering, setting a very stringent constraint to the correct microscopic understanding of the magnetism. These results have been considered as direct evidence against [6] the above local Heisenberg picture and against [5] the alternative spin-density-wave picture for itinerant electrons with nesting Fermi surface [6–10]. Clearly, a comprehensive new picture is urgently needed to explain the microscopic origin of the magnetic structure together with the observed strong anisotropy, and, in particular, to address the additional symmetry breaking, considering its profound implications to the electronic structure and the superconductivity.

In this Letter, we report a first-principles Wannier function analysis [16,17] of the electronic structure of the representative parent compound, LaOFeAs. A purely electronic ferro-orbital order is found to spontaneously break the rotational symmetry and drive the observed magnetic and structural transitions without resorting to the widely employed Fermi surface nesting or magnetic frustration. In great contrast to the cuprates, our study reveals the essential roles of the orbital degree of freedom (especially its short-range correlation) in the electronic structure of iron pnictides. In particular, the expected light mass of orbiton and its strong coupling to the magnon advocate its active roles in magnon decay and electron pairing.

The electronic structure of LaOFeAs is calculated within local spin density approximation (LSDA) and its local interaction extension (LDA + U) of density functional theory, implemented via full potential, all-electron, line-

arized augmented plane wave basis [18]. The atomic positions are relaxed at the experimental lattice constants of the undistorted lattice at 175 K [3]. A unit cell containing four Fe atoms in the plane is adopted to accommodate the observed C-AF structure. The x axis is chosen along the AFM ordered direction of C-AF. A set of energy-resolved symmetry-respecting Wannier functions (WFs) is then constructed [16,17] that spans the complete Hilbert space within 3 eV of the Fermi level.

In significant contrast to the maximally localized WF method [19] used in the previous studies [10,20], our construction exploits the "gauge freedom" [19] of the WFs to achieve localization within constraints of the point-group symmetry [16,17]. Specifically, the cores of our Fe d_{xz} and d_{yz} WFs extend toward the directions of the magnetic ordering, not the As atoms. Consequently, the one-particle density matrix, $\rho_{ij} = \langle \mathrm{WF}_i | \hat{\rho} | \mathrm{WF}_j \rangle$, is locally diagonalized automatically, allowing direct detection of *spontaneous* orbital polarization [21].

Illustrated in Fig. 1(a) are two of the resulting WFs most relevant to our further analysis (Fe $3d_{xz}$ and $3d_{yz}$), as they are the only d-orbitals anisotropic in the xy directions. To simplify the visualization, a sketch illustration of these WFs at the two neighboring sites is given in Fig. 1(b). The dramatic effects of hybridizing with tetrahedral positioned As $4p$ orbitals can be clearly observed from the antibonding "tails" of the WFs. Notice, in particular, how such hybridization bends the tails of the WFs *perpendicular* to their original directions, and significantly modifies the local point-group symmetry. In great contrast to the normal two-dimensional character, the d_{xz} and d_{yz} WFs present a clasplike shape around the iron center.

With the help of these WFs, the LSDA band structures for nonmagnetic (NM) and C-AF LaOFeAs are compared in Fig. 2. To explicitly illustrate the effects of broken periodicity, the band structures are presented in the reciprocal space of the nominal NM unit cell containing only two Fe atoms. In this representation, additional gap openings and "shadow bands" can be clearly observed in the C-AF case, whose intensity reflects the strength of these bands' coupling to the magnetic order.

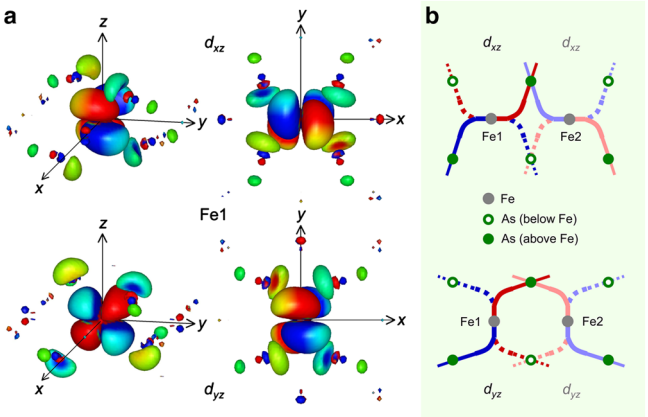

FIG. 1 (color online). (a) Side view (left) and top view (right) for the Fe1 $3d_{xz}$ (upper panels) and $3d_{yz}$ (lower panels) Wannier orbitals obtained from nonmagnetic calculations, colored by their positive (red) and negative (blue) gradient. (b) Sketches of top view of these orbitals on two nearest-neighboring Fe atoms along the x direction (Fe1 and Fe2). The solid (dashed) lines denote the tails above (below) the Fe plane.

Notice that the bands near the Fermi level (zero energy) primarily consist of the above mentioned Fe d_{xz} and d_{yz} WFs (cf. Fig. 1). In the NM case, these two orbitals are degenerate as guaranteed by the point-group symmetry. In the C-AF case, on the other hand, a very large splitting in the broad vicinity of the Fermi level is observed involving the d_{yz} orbital, while the d_{xz} orbital is only weakly affected. This indicates that *only one* of the two orbitals is significantly involved in the magnetic coupling in the C-AF configuration, and the symmetry between the orbitals is broken. Indeed, as the magnetic order develops, the spin polarization (obtained from ρ_{ij}) is found to be much stronger in the d_{yz} orbital ($\sim 0.34\mu_B$) than in the d_{xz} orbital ($\sim 0.15\mu_B$), due to its loss of electron occupation in the spin minority channel. Introduction of a realistic moderate local interaction ($U = 2$ eV and $J_H = 0.5$ eV) further enhances this effect and increases the Fe d_{yz} polarization to $0.58\mu_B$, while the moment in the Fe d_{xz} remains small ($0.23\mu_B$) with both spin channels heavily populated.

In addition, the gap opening, Δ, of the d_{yz} orbital is found to be *comparable* to the band width, W, as shown in Fig. 2. Such a large gap is commonly encountered in strongly correlated systems where the magnetism is more conveniently described by interacting local moments, rather than itinerant electrons with nested Fermi surface. Therefore, we will proceed below to build a local correlated picture for the electronic structure.

Further insights into the microscopic local processes are revealed by transforming the DFT Hamiltonian of the NM case to the Wannier basis, as given in Table I. Unexpectedly, the leading hopping paths of Fe d_{yz} orbital are to the neighboring d_{yz} and $d_{x^2-y^2}$ orbitals along the x direction, *perpendicular to its original direction*. This is anti-intuitive since within the simple cubic symmetry the former would have been very weak "π-bond"-like, while

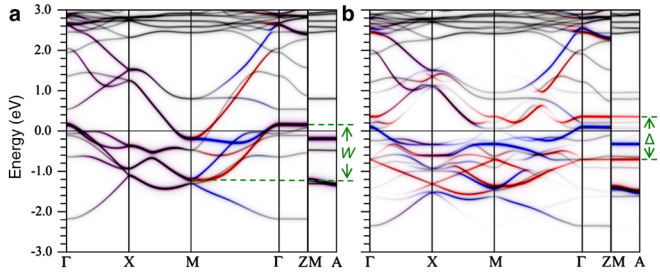

FIG. 2 (color online). Electronic band structures of (a) nonmagnetic and (b) C-AF configurations, represented in the nonmagnetic Brillouin zone. The weight of the Wannier Fe $3d_{xz}$ and $3d_{yz}$ orbitals are presented via blue and red colors, respectively.

TABLE I. Onsite energy (first row) and hopping integrals among Fe 3d Wannier orbitals for the nonmagnetic case (in eV). Fe2 and Fe3 are the NN and NNN of Fe1 (cf. Fig. 3).

⟨WFs|H|WFs⟩	Fe1 z^2	x^2-y^2	yz	xz	xy
Fe1 ϵ-μ	−0.03	−0.20	0.10	0.10	0.34
Fe2 z^2	0.13	0.31	−0.10	0.00	0.00
Fe2 x^2-y^2	0.31	−0.32	**0.42**	0.00	0.00
Fe2 yz	−0.10	0.42	**−0.40**	0.00	0.00
Fe2 xz	0.00	0.00	0.00	**−0.13**	−0.23
Fe2 xy	0.00	0.00	0.00	−0.23	−0.30
Fe3 z^2	0.06	0.00	−0.08	0.08	0.26
Fe3 x^2-y^2	0.00	−0.10	0.12	0.12	0.00
Fe3 yz	0.08	−0.12	**0.25**	−0.07	−0.05
Fe3 xz	−0.08	−0.12	−0.07	0.25	0.05
Fe3 xy	0.26	0.00	0.05	−0.05	0.16

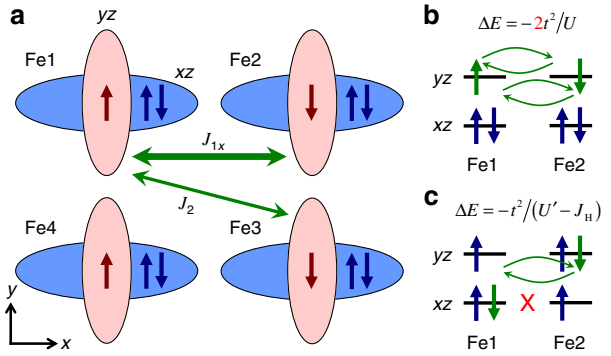

FIG. 3 (color online). (a) Schematic of C-AF magnetic structure with highly anisotropic NN coupling due to orbital ordering. (b), (c) The kinetic energy ΔE in the ferro-orbital and staggered-orbital structures. t and U denote the hopping parameter and intraorbital Coulomb repulsion, while U' and J_H denote the interorbital repulsion and Hund's exchange, respectively.

the latter would have been symmetry forbidden and identical to zero. By contrast, the supposedly stronger "σ-bond"-like NN $d_{xz} - d_{xz}$ hopping along the x direction is remarkably weak. These features are qualitatively different from those used in the previous studies [22,23]. Our distinctly different results originate mathematically from the change of direction in the WFs' hybridization tails, as visualized above in Fig. 1 [21]. Physically, this reflects the dramatic influence of the tetrahedral positioning of As 4p orbitals on the Fe 3d orbitals, and reveals the importance of As atom positions and Fe-As phonon modes in the electronic structure in general.

A simple "minimal" picture of the low-energy physics now emerges from the above analysis that elucidates the nature of C-AF magnetic structure together with the observed large anisotropy. Let us again focus only on the Fe d_{xz} and d_{yz} orbitals. As illustrated in Fig. 3, given almost doubly-occupied Fe d_{xz} orbitals and almost singly-occupied, spin-polarized Fe d_{yz} orbitals, the d_{yz} orbitals prefer AFM alignments along the directions of the efficient hopping, to benefit from the kinetic energy (the "superexchange"). Within the oversimplified strong coupling limit [21] to the second order in the hopping parameters in Table I, the leading AFM magnetic couplings among the d_{yz} subspace are the NN coupling along the x direction, J_{1x}, and the NNN coupling, $J_2 \sim 0.4J_{1x}$. In comparison, the NN coupling along the y direction, $J_{1y} \sim 0.1J_{1x}$, is insignificant. This large anisotropy is in good agreement with the current experimental [5] and theoretical observations [15]. Clearly, the anisotropy *owes its origin to the orbital degree of freedom*, as the rotational symmetry is broken upon orbital polarization. Therefore, modeling the magnetic structure with a standard Heisenberg model [4,5,12–15] would suffer from its very limited applicability [24], as it lacks flexibility to break the rotational symmetry spontaneously, or to adjust the magnetic coupling strength according to the orbital structure.

As shown in Fig. 3, following these two leading AFM couplings J_{1x} and J_2, the observed C-AF structure is naturally established *locally*, without resorting to Fermi surface nesting. The seemingly ferromagnetic alignment along the y axis results primarily from the NN and NNN AFM alignment across the columns. Contrary to previous theoretical explanation [12–14], in our picture the observed C-AF structure is *not* frustrated or competing with any other magnetic structure (e.g.: G-AF), and thus can sustain a high transition temperature [3].

In order to maximize the kinetic energy gain via the superexchange processes, the orbitals not only have to be polarized, but also need to be ordered. (Other magnetic/orbital configurations were found to have higher energies.) Indeed, in the above picture, all the sites are polarized the same way with the d_{yz} orbital being less occupied and more spin polarized. This can be considered an example of "ferro-orbital order" [22,25]. The formation of this rare orbital order can be understood by noting the anti-intuitive NN hopping path along the x direction (cf. Table I), dominated by only hopping between d_{yz} orbitals without d_{xz}-d_{yz} cross hopping. As illustrated in Fig. 3(b), the best way to utilize the kinetic energy in this case is indeed the ferro-orbital, AFM magnetic alignment, since one electron from *both* sites benefit from the kinetic energy. In comparison, the more common staggered-orbital, ferromagnetic alignment (e.g., in undoped manganites) can utilize efficient hoppings in *only one* channel [cf. Fig. 3(c)], despite the additional benefit from the intra-atomic interactions [21]. That is, the unique hopping path leads to a rare ground state of the undoped iron pnictides consisting of cooperative ferro-orbital and C-AF orders.

The ferro-orbital phase is in fact directly responsible for the tetragonal-to-orthorhombic lattice transition observed at $T_s \sim 155$ K [3]. As soon as long-range ferro-orbital order takes place at T_{OO} ($=T_s$), d_{xz} orbitals becomes more occupied macroscopically (cf. Fig. 3), leading to a longer bond in the x direction, in agreement with the experiment [26]. In general, it is very rare to have AFM bond longer than the ferromagnetic one in the late transi-

tion metal compounds, since the AFM superexchange grows on almost half-filled orbitals (with less charge). In iron pnictides, this unusual long bond is realized only because of the perpendicular extension of the hybridization tails discussed above. This subtle behavior distinguishes our result from a previous study [22], in which the AFM bond is less populated and thus would be shorter.

It is important to further clarify the weak coupling strength between the elastic lattice distortion and the orbital order. When the lattice is set to frustrate the orbital order in our calculation by exchanging the lattice constants in the x and y directions, only less than 10 meV cost per Fe is found, an order of magnitude smaller than the superexchange energy. In essence, the orbital order originates almost entirely from the *electronic energy*, and the lattice simply follows the orbital order. On the other hand, such a weak coupling should allow a strong short-range orbital correlation even above T_s, offering a natural explanation to the large anomalous signal extending to 40 K above T_s in the thermal expansion measurement [27].

Since it is the same kinetic energy gain that drives both the magnetic and orbital orders, they are thus strongly coupled to each other, as in the Kugel-Khomskii model [25]. This is the natural reason for the close proximity of observed T_N and T_s. Unlike the manganites, where the orbital order is further stabilized by the large lattice-orbital coupling $\sim$0.9 eV [17], the weak coupling to the elastic lattice mode here does not help raising T_s noticeably from T_N. This suggests a light effective mass of the orbiton, comparable to the magnon mass. Thus, an intimate relationship between the excitations in the spin and orbital channel is expected. Indeed, an efficient orbiton-assisted decay offers a very interesting possible explanation to the observed large line width of magnon at large momentum [5]. Furthermore, the controlling role of Fe-As-Fe positioning in the unconventional hopping implies large isotope effects in both magnetic [28] and orbital transitions.

Our study also has several implications on the high-temperature superconductivity of doped iron pnictides. In great contrast to the cuprates, our results reveal the essential roles of the orbital degree of freedom in iron pnictides. Upon doping, the long-range magnetic and orbital orders would naturally perish rapidly through the disruption of the above superexchange process by doping-induced charge fluctuation. (Recall that the above process maximizes with three electrons in the xz/yz complex in average.) Nonetheless, the short-range orbital correlation should persist deep into the underdoped superconducting regime. In addition, the light mass of orbiton and its strong coupling to the magnon make orbiton another interesting participant in the pairing mechanism. Furthermore, the correlated nature suggested by our study indicates a much stronger local electron-boson coupling than the current mean-field estimation [29]. Finally, our correlated picture also supports a strong coupling nature of superconductivity (with strong phase fluctuation) in the underdoped regime, in agreement with the recent observation of low superfluid density [30] with relatively high T_c.

In summary, with our first-principles Wannier function analysis, a rare ferro-orbital order is identified in LaOFeAs that breaks the rotational symmetry and gives rise to the recently observed giant anisotropy of magnetic coupling in undoped iron pnictides. The observed magnetic and lattice structures result *locally*—without widely applied frustration or the need for Fermi surface nesting. In great contrast to the cuprates, our study reveals the essential roles of the orbital degree of freedom in iron pnictides in general, and suggests active roles of light orbiton in magnon decay and electron-pairing. Finally, the pure electronic origin and the large coupling strength advocate a correlated nature of undoped iron pnictides, and support the notion of strong coupling superconductivity in the underdoped regime.

This work was supported by the U.S. Department of Energy, Office of Basic Energy Science, under Contract No. DE-AC02-98CH10886, and DOE-CMSN.

[1] P. A. Lee *et al.*, Rev. Mod. Phys. **78**, 17 (2006).
[2] Y. Kamihara *et al.*, J. Am. Chem. Soc. **130**, 3296 (2008).
[3] C. de la Cruz *et al.*, Nature (London) **453**, 899 (2008).
[4] Z. P. Yin *et al.*, Phys. Rev. Lett. **101**, 047001 (2008).
[5] J. Zhao *et al.*, Nature Phys. **5**, 555 (2009).
[6] I. I. Mazin *et al.*, Phys. Rev. B **78**, 085104 (2008).
[7] F. Wang *et al.*, Phys. Rev. Lett. **102**, 047005 (2009).
[8] J. Dong *et al.*, Europhys. Lett. **83**, 27006 (2008).
[9] S. Raghu *et al.*, Phys. Rev. B **77**, 220503(R) (2008).
[10] K. Kuroki *et al.*, Phys. Rev. Lett. **101**, 087004 (2008).
[11] A. Moreo *et al.*, Phys. Rev. B **79**, 134502 (2009).
[12] Q. Si and E. Abrahams, Phys. Rev. Lett. **101**, 076401 (2008).
[13] C. Fang *et al.*, Phys. Rev. B **77**, 224509 (2008).
[14] T. Yildirim, Phys. Rev. Lett. **101**, 057010 (2008).
[15] M. J. Han *et al.*, Phys. Rev. Lett. **102**, 107003 (2009).
[16] W. Ku *et al.*, Phys. Rev. Lett. **89**, 167204 (2002).
[17] W.-G. Yin *et al.*, Phys. Rev. Lett. **96**, 116405 (2006).
[18] K. Schwarz *et al.*, Comput. Phys. Commun. **147**, 71 (2002).
[19] N. Marzari and D. Vanderbilt, Phys. Rev. B **56**, 12 847 (1997).
[20] C. Cao *et al.*, Phys. Rev. B **77**, 220506(R) (2008).
[21] See EPAPS Document No. E-PRLTAO-104-027001 for supplementary material. For more information on EPAPS, see http://www.aip.org/pubservs/epaps.html.
[22] F. Krüger *et al.*, Phys. Rev. B **79**, 054504 (2009).
[23] M. J. Calderón *et al.*, New J. Phys. **11**, 013051 (2009).
[24] A. N. Yaresko *et al.*, Phys. Rev. B **79**, 144421 (2009).
[25] K. I. Kugel' and D. I. Khomskii, Zh. Eksp. Teor. Fiz. **15**, 629 (1972) [JETP Lett. **15**, 446 (1972)].
[26] Q. Huang *et al.*, Phys. Rev. B **78**, 054529 (2008).
[27] L. Wang *et al.*, Phys. Rev. B **80**, 094512 (2009).
[28] R. H. Liu *et al.*, Nature (London) **459**, 64 (2009).
[29] L. Boeri *et al.*, Phys. Rev. Lett. **101**, 026403 (2008).
[30] H. Luetkens *et al.*, Phys. Rev. Lett. **101**, 097009 (2008).